Article

Catalytic Reaction Mechanism of Homogentisate Dioxygenase: A Hybrid DFT Study

Tomasz Borowski, Valentin Georgiev, and Per E. M. Siegbahn

J. Am. Chem. Soc., **2005**, 127 (49), 17303-17314• DOI: 10.1021/ja054433j • Publication Date (Web): 17 November 2005

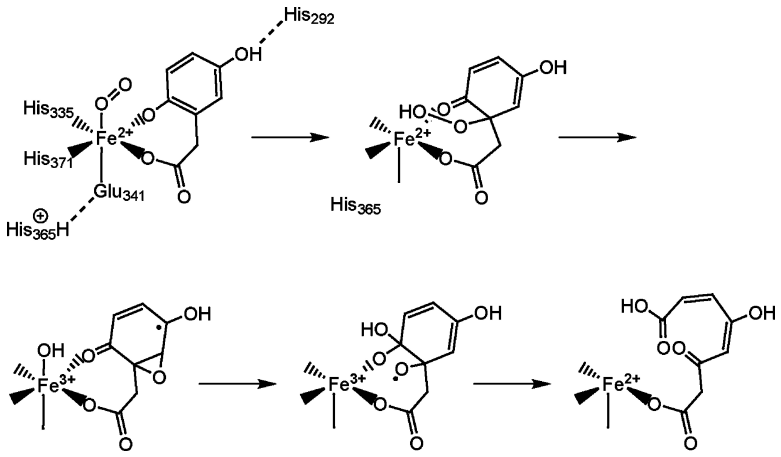

More About This Article

Additional resources and features associated with this article are available within the HTML version:

- Supporting Information
- Links to the 3 articles that cite this article, as of the time of this article download
- Access to high resolution figures
- Links to articles and content related to this article
- Copyright permission to reproduce figures and/or text from this article

View the Full Text HTML

J|A|C|S
ARTICLES
Published on Web 11/17/2005

Catalytic Reaction Mechanism of Homogentisate Dioxygenase: A Hybrid DFT Study

Tomasz Borowski,* Valentin Georgiev, and Per E. M. Siegbahn

Contribution from the Department of Physics, Stockholm Center for Physics, Astronomy and Biotechnology, Stockholm University, S-106 91 Stockholm, Sweden

Received July 5, 2005; E-mail: borowski@physto.se

Abstract: Human homogentisate dioxygenase is an Fe^{II}-dependent enzyme responsible for aromatic ring cleavage. The mechanism of its catalytic reaction has been investigated with the hybrid density functional method B3LYP. A relatively big model of the active site was first used to determine the substrate binding mode. It was found that binding of the substrate dianion with a vacant position trans to Glu341 is most favorable. The model was then truncated to include only the most relevant parts of the active-site residues involved in iron coordination and substrate binding. Thus, methylimidazole was used to model His292, His335, His365, and His371, while propionate modeled Glu341. The computational results suggest that the catalytic reaction of homogentisate dioxygenases involves three major chemical steps: formation of the peroxo intermediate, homolytic cleavage of the O−O bond leading to an arene oxide radical, and finally, cleavage of the six-membered ring. Calculated barriers for alternative reaction paths are markedly higher than for the proposed mechanism, and thus the computational results successfully explain the product specificity of the enzyme. Interestingly, the results indicate that the type of ring scission, *intra* or *extra* with respect to the substituents coordinating to iron, is controlled by the barrier heights for the decay of the arene oxide radical intermediate.

I. Introduction

Homogentisate dioxygenase (HGD) is an Fe^{II}-dependent enzyme involved in the catabolism of tyrosine and phenylalanine in human.[1] It catalyzes the oxidative ring scission of homogentisate (HG) to maleylacetoacetate, which means that the aromatic ring is specifically cleaved between the carbons substituted with hydroxyl and carboxymethyl groups (C1 and C2, see Scheme 1). This type of ring cleavage resembles the reaction catalyzed by Fe^{III}-dependent intradiol dioxygenases, which cleave catechol rings between the carbon atoms binding hydroxyl groups. However, the dependence on Fe^{II} and the structure of the active site (vide infra) indicate that HGD is more related to the extradiol dioxygenases, which cleave the catechol ring at a bond adjacent to the carbons binding the hydroxyl groups. The literature on both types of diol dioxygenases is very rich, and we refer interested readers to excellent reviews on the subject.[2−8]

Among the enzymes characterized thus far, HGD, gentisate 1,2-dioxygenase (GD)[9,10] and the recently discovered salicylate 1,2-dioxygenase (SalD)[11,12] catalyze very similar reactions (see Scheme 2). GD is involved in the oxidative ring scission of gentisate, which differs from HG by having a carboxyl instead of carboxymethyl substituent. Otherwise, the reactions of HGD and GD are very similar. On the other hand, SalD cleaves salicylate, which may be considered to be a derivative of gentisate, lacking the C4 hydroxyl group. Interestingly, the product of salicylate oxidation has a trans configuration around one of the double bonds (C3−C4). This observation is thought provoking, since the lack of the C4-bound hydroxyl group prevents any keto−enol tautomerization, which might explain this rotation around the double bond.

Scheme 1. Reaction Catalyzed by Homogentisate Dioxygenase

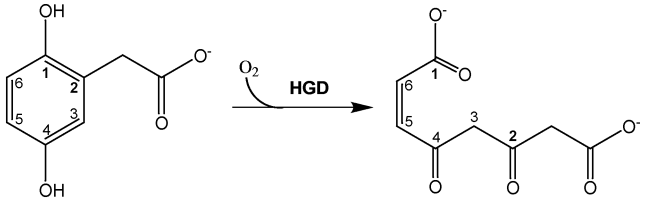

homogentisate (HG) maleylacetoacetate

From the medical perspective, HGD is an important enzyme connected with two metabolic disorders. First, the deficiency of HGD activity elicits alkaptonuria, a rare hereditary human disease.[13] Mutations within the HGD gene inactivate the enzyme leading to elevated levels of HG which, when oxidized,

(1) Knox, W. E.; Edwards, S. W. *J. Biol. Chem.* **1955**, *216*, 479−487.
(2) Costas, M.; Mehn, M. P.; Jensen, M. P.; Que, L. *Chem. Rev.* **2004**, *104*, 939−986.
(3) Que, L., Jr.; Ho, R. Y. N. *Chem. Rev.* **1996**, *96*, 2607−2624.
(4) Ryle, M. J.; Hausinger, R. P. *Curr. Opin. Chem. Biol.* **2002**, *6*, 193−201.
(5) Bugg, T. D. H. *Tetrahedron* **2003**, *59*, 7075−7101.
(6) Bugg, T. D. H. *Curr. Opin. Chem. Biol.* **2001**, *5*, 550−555.
(7) Bugg, T. D. H.; Winfield, C. J. *Nat. Prod. Rep.* **1998**, 513−530.
(8) Solomon, E. S.; Brunold, T. C.; Davis, M. I.; Kemsley, J. N.; Lee, S. K.; Lehnert, N.; Neese, F.; Skulan, A. J.; Yang, Y. S.; Zhou, J. *Chem. Rev.* **2000**, *100*, 235−349.
(9) Harpel, M.; Lipscomb, J. *J. Biol. Chem.* **1990**, *265*, 22187−22196.
(10) Harpel, M.; Lipscomb, J. *J. Biol. Chem.* **1990**, *265*, 6301−6311.
(11) Hintner, J.; Lechner, C.; Riegert, U.; Kuhm, A.; Storm, T.; Reemtsma, T.; Stolz, A. *J. Bacteriol.* **2001**, *183*, 6936−6942.
(12) Hintner, J.-P.; Reemtsma, T.; Stolz, A. *J. Biol. Chem.* **2004**, *279*, 37250−37260.

Scheme 2. Reaction Catalyzed by: (A) Gentisate 1,2-Dioxygenase (GD) and (B) Salicylate 1,2-Dioxygenase (SalD)

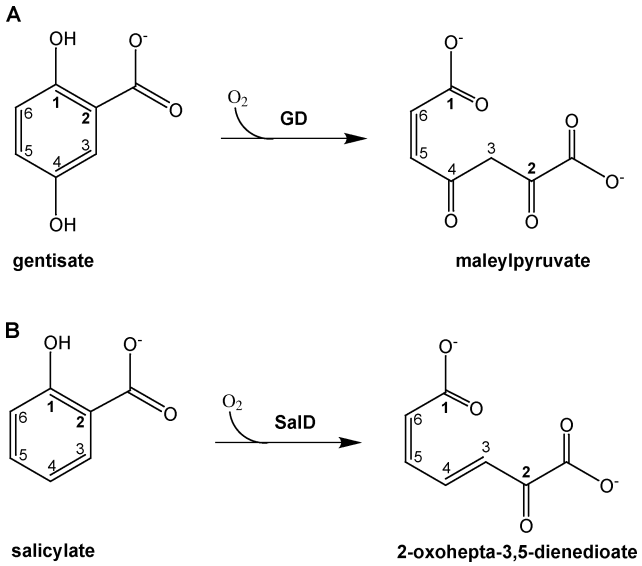

polymerizes to the product known as the ochronotic pigment. This substance accumulates in connective tissue and causes degenerative arthritis.[14,15] The second metabolic disorder is tyrosinemia type I which is a life-threatening disease caused by dysfunction of fumarylacetoacetase, an enzyme located downstream from HGD in the tyrosine catabolic pathway. Currently, tyrosinemia type I is treated with inhibitors of 4-hydroxyphenylpyruvate dioxygenase (4-HPPD), an enzyme preceding HGD.[16]

Despite the considerable importance of HGD, only recently was some progress made in the research on this interesting enzyme. The crystal structure of human HGD in the apo and Fe-bound state was solved by Titus and co-workers.[17] The crystal structure shows that monomers of HGD associate tightly to form a homohexameric structure which was described as a dimer of trimers. Each monomer has its active site located in the proximity of the intersubunit interface. As in other extradiol dioxygenases, the active-site iron is coordinated by two histidines (His335, His371) and one glutamate (Glu341), which form the 2-his-1-carboxylate facial triad occupying one face of the metal coordination octahedron, a motif found in many Fe^{II}-dependent enzymes.[18] The other three coordination positions around iron are available for homogentisate and dioxygen or solvent ligands. In addition to this iron-binding motif, several other residues were proposed to be involved in substrate binding and/or catalysis. First, His365 forms a hydrogen bond with Glu341 and may be involved in substrate deprotonation upon binding. Second, His292 was proposed to form a hydrogen bond with the C4-bound hydroxyl group of HG, and together with Pro295, Pro332, and Tyr333 forms a solvent-accessible box, which was also implicated for the substrate binding.

Concerning the biochemical studies on HGD, a recently published kinetic analysis has provided firm evidence for an ordered mechanism, in which HG binds first to the enzyme followed by a dioxygen reacting with the Fe^{II}−HGD−HG complex.[19,20] Furthermore, an optimum pH (6.2) and a turnover number (16 s^{-1}) were measured. Aside from this, little is known about the catalytic mechanism of HGD. Owing to the similarity between the reactions catalyzed by HGD and GD, it was argued[17] that the HGD mechanism should parallel that proposed for GD.[9,10] This mechanism is presented in Scheme 3, and with the exception for the chemical identity of the substrate and the involvement of His292, it is very similar to the mechanism proposed by Lipscomb and co-workers for extradiol dioxygenases.[21,22] Thus, it is proposed that HG chelates Fe^{II} with its carboxyl and deprotonated hydroxyl groups. An analogous binding mode was confirmed in spectroscopic studies on GD.[9] The deprotonation of one of the hydroxyl groups on binding to the Fe^{II} is well documented in the literature,[23−25] and therefore, it seems very likely to take place also in the case of HGD. Molecular dioxygen reacts with this HGD−HG complex and forms a peroxo intermediate with an O−O bridge joining the C2 carbon and Fe^{II}. In the next step, the peroxo intermediate undergoes a Criegee rearrangement, yielding a seven-membered lactone ring, protonated His292, and a hydroxyl group bound to Fe^{II}. Finally, the lactone ring is hydrolyzed to an enol form of the product, maleylacetoacetate. In relation to this last step, there is experimental evidence that one of the extradiol dioxygenases possesses a catalytic activity for lactone hydrolysis.[26] Moreover, the isotope-labeling experiments reported in the same work demonstrated that oxygen of the carboxyl group originates partly from molecular dioxygen and partly from water. These findings were interpreted in favor of the formation of the lactone intermediate during the extradiol ring cleavage.[26] However, there are also some recent experimental data which are difficult to explain with such a generic mechanism for Fe^{II}-dependent extradiol dioxygenases. More specifically, the discovery of salicylate 1,2-dioxygenase and the observed stereochemistry of its product (trans configuration around the C3−C4 bond) show that the substrate does not have to possess the second hydroxyl group (or its equivalent) and that the ring scission mechanism is probably more complicated, at least for this particular dioxygenase.[11,12]

Recently, the results of two independent DFT investigations of the catalytic mechanism of the extradiol dioxygenases were published. In the first study, Deeth and Bugg reached a conclusion that the bridging peroxo species is not a stable intermediate but rather a transition state leading directly form

(13) La Du, B. N.; Zannoni, V. G.; Laster, L.; Seegmiller, J. E. *J. Biol. Chem.* **1958**, *230*, 251−260.
(14) Fernández-Cañón, J.; Granadino, B.; de Bernabé, D. B.-V.; Renedo, M.; Fernández-Ruiz, E.; Peñalva, M.; de Córdoba, S. R. *Nat. Genet.* **1996**, *14*, 19−24.
(15) Rodriguez, J. M.; Timm, D. E.; Titus, G. P.; de Bernabé D. B.-V.; Criado, O.; Mueller, H. A.; de Córdoba, S. R.; Peñalva, M. A. *Hum. Mol. Genet.* **2000**, *9*, 2341−2350.
(16) Lindstedt, S.; Holme, E.; Lock, E. A.; Hjalmarson, O.; Strandvik, B. *Lancet* **1992**, *340*, 813−817.
(17) Titus, G.; Mueller, H.; Burgner, J.; Córdoba, S. R. D.; Peñalva, M.; Timm, D. *Nat. Struct. Biol.* **2000**, *7*, 542−546.
(18) Que, L. *Nat. Struct. Biol.* **2000**, *7*, 182−184.
(19) Amaya, A. A.; Brzezinski, K. T.; Farrington, N.; Moran, G. R. *Arch. Biochem. Biophys.* **2004**, *421*, 135−142.
(20) Veldhuizen, E. J. A.; Vaillancourt, F. H.; Whiting, C. J.; Hsiao, M. M.-Y.; Gingras, G.; Xiao, Y.; Tanguay, R. M.; Boukouvalas, J.; Eltis, L. D. *Biochem. J.* **2005**, *386*, 305−314.
(21) Arciero, D.; Lipscomb, J. *J. Biol. Chem.* **1986**, *261*, 2170−2178.
(22) Groce, S. L.; Miller-Rodeberg, M. A.; Lipscomb, J. D. *Biochemistry* **2004**, *43*, 15141−15153.
(23) Sato, N.; Uragami, Y.; Nishizaki, T.; Takahashi, Y.; Sazaki, G.; Sugimoto, K.; Nonaka, T.; Masai, E.; Fukuda, M.; Senda, T. *J. Mol. Biol.* **2002**, *321*, 621−636.
(24) Uragami, Y.; Senda, T.; Sugimoto, K.; Sato, N.; Nagarajan, V.; Masai, E.; Fukuda, M.; Mitsu, Y. *J. Inorg. Biochem.* **2001**, *83*, 269−279.
(25) Vaillancourt, F. H.; Barbosa, C. J.; Spiro, T. G.; Bolin, J. T.; Blades, M. W.; Turner, R. F. B.; Eltis, L. D. *J. Am. Chem. Soc.* **2002**, *124*, 2485−2496.
(26) Sanvoisin, J.; Langley, G. J.; Bugg, T. D. H. *J. Am. Chem. Soc.* **1995**, *117*, 7836−7837.

Scheme 3. Reaction Mechanism Proposed by Titus et al.[17] for Homogentisate Dioxygenase

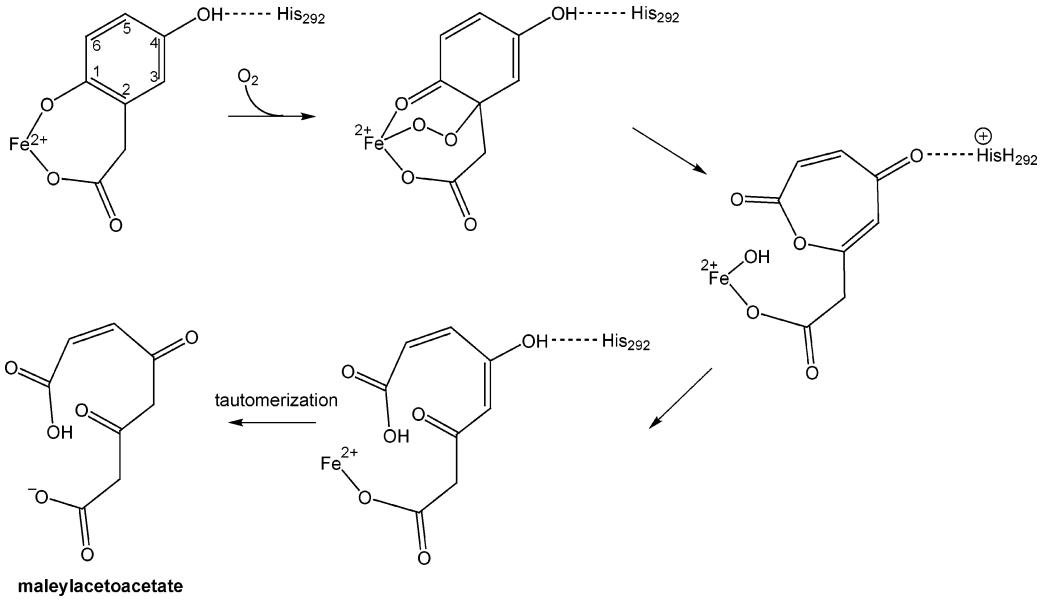

the ternary enzyme−catechol−dioxygen complex to Fe^{IV}−OH/arene oxide intermediate.[27] The lowest barrier was found on the quintet potential energy surface, where the ground state of the reactant has a doubly deprotonated catechol and a singly protonated dioxygen ligand, i.e., hydroperoxo group, coordinated to iron. The attack of the OOH group on the ring is assisted by a carboxylate, i.e. one of the iron ligands, which transiently accepts a proton from the hydroperoxo group, as the oxygen−carbon bond develops. Arene oxide, formed in this reaction, opens to the lactone ring, which is hydrolyzed in the last step of the catalytic cycle. In the second work, Siegbahn and Haeffner found a stable, bridging peroxo structure, which in a homolytic O−O bond cleavage yields an alkoxyl radical intermediate.[28] The latter collapses (activation barrier of 0.2 kcal/mol) to an Fe^{III}−OH/arene oxide radical species, which later opens to a seven-membered lactone radical ring. The attack of the Fe^{III}-bound OH radical on this ring initiates the formation of the final product.

In this contribution the results of hybrid DFT calculations for the mechanism of the catalytic reaction of HGD are reported. On the basis of the results obtained for a more complete model of the active site, the substrate binding mode is proposed. The mechanism of the HGD catalytic reaction was then studied with a smaller model. The computational results indicate that, once the peroxo intermediate is formed, homolytic cleavage of the O−O bond leads to a radical arene oxide, which then decays to the final product without the intermediacy of the seven-membered ring structure. The calculated barriers for the suggested mechanism and some alternative reactions provide an explanation for the observed product specificity of HGD. Finally, the novel part of the mechanism, i.e. the decay of the arene oxide radical, provides new insight into the factors governing the product specificity of aromatic ring-cleaving dioxygenases.

II. Computational Details

The models of the HGD active site are based on the crystal structure solved for the Fe-bound form of the enzyme (PDB code: 1EY2). Two models differing in size have been employed in the calculations. First, a large system (134 atoms, see Figure 1) was used, comprising the iron first-shell ligands (His335, His371, Glu341, and HG), two second-shell histidines (His292 and His365), and three groups defining a substrate box (Pro295, Pro332, and Tyr333). Histidines are modeled with ethylimidazole, and glutamate is modeled with a butyric acid anion, while for prolines and tyrosine only the rings are included in the model. Bonds being cut have been saturated with hydrogens. HG is assumed to be a dianion, His365 is doubly protonated (cation), while His292 is neutral and accepts a hydrogen bond from the phenolic group of HG. The total charge of the model is zero. Restrained optimization has been performed with the atoms corresponding to Cα and Cβ in the His and Glu residues constrained to their positions in the crystal structure. For the models of the proline and tyrosine rings, the positions of all non-hydrogen atoms have been constrained. This large model has been used to study possible binding modes of HG at the active site of HGD.

The second, smaller model (80 atoms) was used to study the reaction mechanism. In this system, the proline and tyrosine rings defining the substrate box were not included. Furthermore, the methyl groups modeling the Cα carbons of the His and Glu residues (drawn in a simple representation in Figure 1) were replaced with hydrogen atoms, and the C−H bond lengths were appropriately adjusted. The positions of these hydrogen atoms and the adjacent carbons (originally Cβ) were constrained in all geometry optimizations. In this way, the rigidity of the protein backbone was taken into account in the model.

All calculations were performed employing hybrid DFT with the B3LYP exchange-correlation functional.[29,30] Two programs, Gaussian03[31] and Jaguar,[32] were used. Geometry optimizations were done with a valence double-ζ basis set coupled with an effective core potential describing the innermost electrons on iron. This particular basis set is labeled lacvp in Jaguar. For the optimized structures the electronic energy was computed with a bigger basis set of triple-ζ quality with polarization functions on all atoms (labeled lacv3p** in Jaguar). The solvent corrections were calculated with the self-consistent reaction field method implemented in Jaguar.[33,34] A dielectric constant

(27) Deeth, R. J.; Bugg, T. D. H. *J. Biol. Inorg. Chem.* **2003**, *8*, 409−418.
(28) Siegbahn, P. E. M.; Haeffner, F. *J. Am. Chem. Soc.* **2004**, *126*, 8919−8932.
(29) Becke, A. D. J. *Chem. Phys.* **1993**, *98*, 5648−5652.
(30) Lee, C.; Yang, W.; Parr, R. G. *Phys. Rev.* **1988**, *B37*, 785−789.
(31) Frisch, M. J. et al. *Gaussian03*, revision B.03; Gaussian Inc.: Pittsburgh, PA, 2003.
(32) *JAGUAR 4.0*; Schrödinger, Inc.: Portland, Oregon, 2000.
(33) Tannor, D. J.; Marten, B.; Murphy, R.; Friesner, R. A.; Sitkoff, D.; Nicholls, A.; Ringnalda, M.; Goddard, W. A., III; Honig, B. *J. Am. Chem. Soc.* **1994**, *116*, 11875−11882.
(34) Marten, B.; Kim, K.; Cortis, C.; Friesner, R. A.; Murphy, R.; Ringnalda, M.; Sitkoff, D.; Honig, B. *J. Phys. Chem.* **1996**, *100*, 11775−11788.

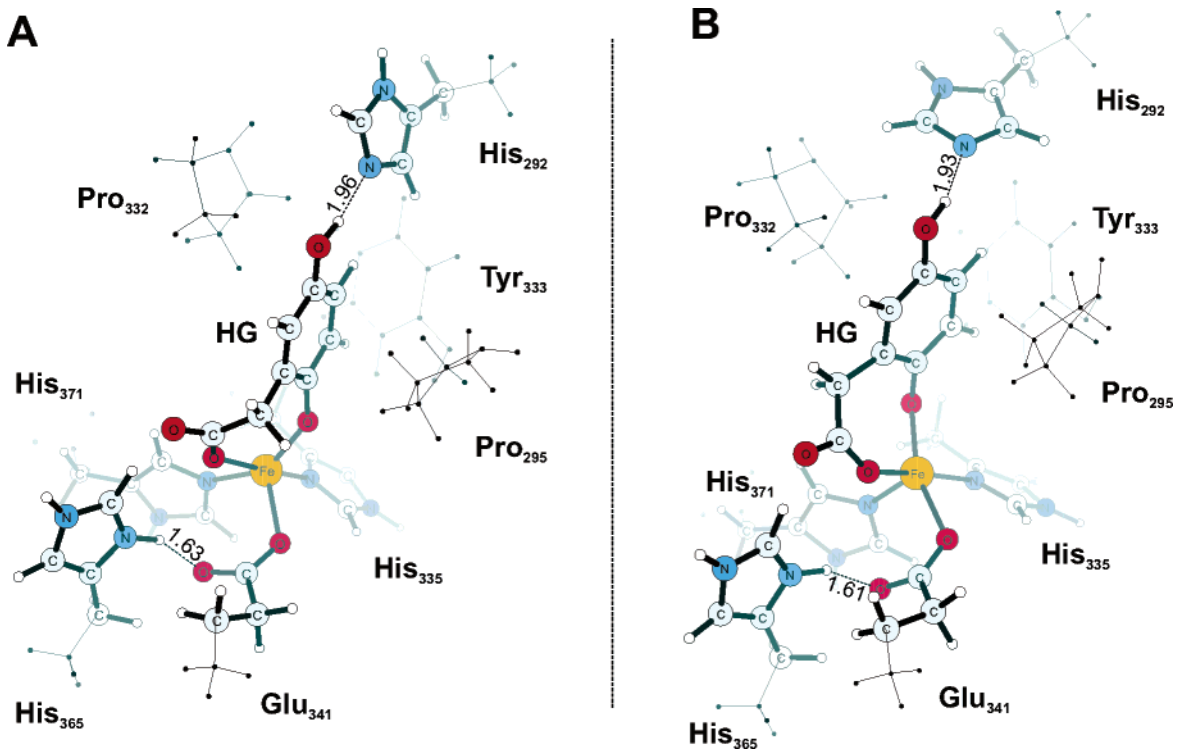

Figure 1. Two possible binding modes for the HG−HGD complex: (A) the lowest-energy configuration with a vacant coordination position trans to Glu341 and (B) the less stable configuration with a vacancy trans to His371. Distances in Å in bold.

of 4 and a probe radius of 1.4 Å were used to model the protein surrounding the active site. Zero energy corresponds to the isolated reactants in their ground states, i.e. the model of the HGD−HG complex in the quintet spin state and the triplet molecular dioxygen.

III. Results and Discussion

The crystal structures available for HGD were solved for an apo and for holo forms of the enzyme, which means that there is currently no structure for the substrate−enzyme complex. For this reason, the first task in the present study was to investigate the structure of the HGD−HG complex. The large model described in Computational Details was used to test possible substrate binding modes, and the results of these investigations are described in the first section below. Then, the results of the studies aiming at the mechanism of the catalytic reaction follow. These calculations have been done with the smaller model of the active site.

Enzyme−Substrate Complex. On the basis of the spectroscopic results for gentisate dioxygenase[9,10] and the available crystal structure of HGD[17] it was proposed that homogentisate binds to the active-site iron through its carboxyl group and the deprotonated C1-bound hydroxyl functionality.[17] The aromatic ring of the substrate should fit into the solvent box defined by Pro295, Pro332, Tyr333, and His292, with His292 accepting a hydrogen bond from the C4-bound hydroxyl group of HG. The structure of the active-site model constructed from the available structural data support only two binding modes presented in Figure 1. More specifically, due to the confined space within the solvent box, the aromatic ring of HG has to be approximately parallel to the prolines and orthogonal to the Tyr333 ring. The binding mode with the substrate and Tyr333 rings stacked together results in steric clashes between the substrate and the prolines. With the HG ring approximately parallel to Pro332 and Pro295, two arrangements around iron are possible. In the first one, the position trans to Glu341 is vacant, and HG occupies sites trans to His335 and His371 (see Figure 1A and also Figure S1). In the second arrangement, the vacancy is trans to His371, and HG is bound at sites trans to Glu341 and His335 (see Figure 1B). The calculated energy difference for these two optimized models is 5.2 kcal/mol in favor of the first one (A). Since this energy splitting remains almost unchanged when the size of the model is reduced (4.9 kcal/mol calculated for the smaller model, which does not include Pro and Tyr residues), it is concluded that the difference comes from the arrangement of the ligands around iron. More specifically, in the less stable configuration, B, the phenolic oxygen of HG binds trans to Glu341, while in the favorable orientation it occupies a position trans to His371. Thus, it is likely that the trans effect governs the arrangement of the ligands around the active-site iron. Interestingly, in the available crystal structures for extradiol dioxygenase−substrate complexes catechol always binds trans to two histidine ligands, leaving the position trans to a carboxylic group for water or NO as an O_2 surrogate.[23−25,35] In conclusion, the proposed binding mode for the HG−HGD complex (Figure 1A) agrees with known structural data obtained for related enzymes. This arrangement around iron is kept in the smaller model used to study the reaction mechanism of HGD.

Finally, we offer a short comment on the expected accuracy of the procedure adopted here to predict the structure of the HG−HGD complex. Homogentisate is a relatively simple aromatic compound with very limited conformational freedom. On the other hand, the geometry of the HGD active site, which is located close to the intersubunit interface, is defined by a tight association between the subunits.[17] Importantly, the geometry of Pro295 and Pro332, which define the box into

(35) Vetting, M. W.; Wackett, L. P.; Que, L.; Lipscomb, J. D.; Ohlendorf, D. H. *J. Bacteriol.* **2004**, *186*, 1945−1958.

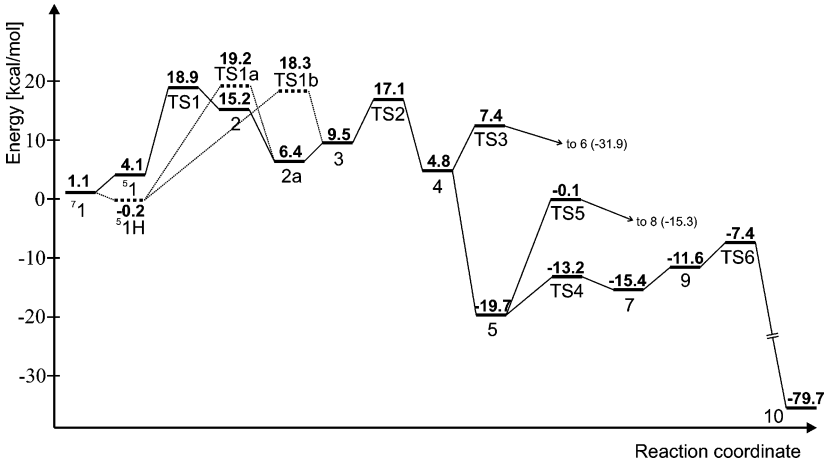

Figure 2. Calculated energy profile along the suggested reaction path for HGD.

Scheme 4. Suggested Mechanism for the Catalytic Reaction of HGD

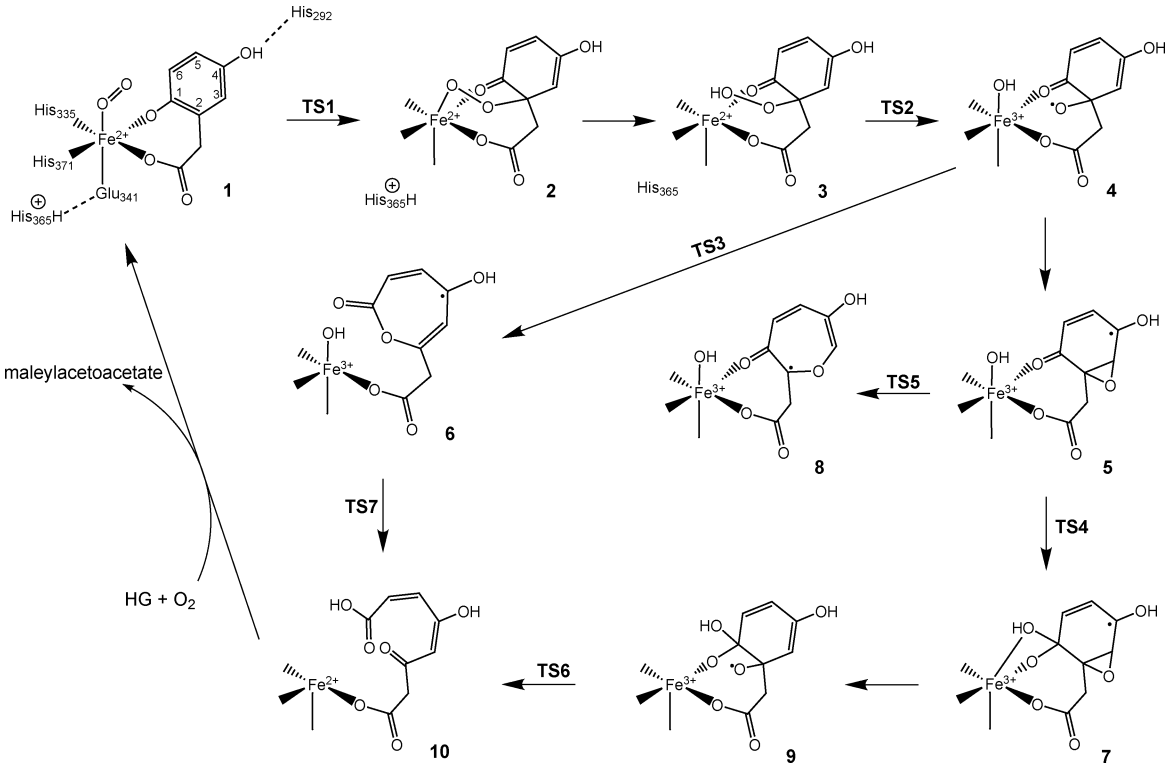

which HG should fit, cannot be changed without affecting the structure of the protein backbone. Finally, the comparison of two crystal structures of homoprotocatechuate 2,3-dioxygenase (Figure S2), solved with (PDB code: 1Q0C) and without (1F1X) substrate bound, shows that the active-site structure undergoes very modest changes upon substrate binding. Taken together, it seems that the relatively simple approach, used here to predict the structure of the HG−HGD complex, and similar to the famous key−lock model, is good enough since both the "key" and the "lock" are relatively rigid.

Reaction Mechanism. From the computational results it follows that the catalytic reaction of HGD involves three major steps (see Scheme 4). First, molecular dioxygen binds to iron trans to Glu341 and reacts with homogentisate, forming the peroxo-bridged intermediate (**1**, **2**, and **3**). The second major step is a homolytic cleavage of the O−O bond in the hydroperoxo intermediate **3**, which leads to the arene oxide radical **5**. These two steps are similar to the corresponding reactions proposed previously for extradiol dioxygenases.[28] Finally, the last phase of the catalytic cycle involves a nucleophilic attack of the Fe-bound OH group on the carbonyl carbon of the arene oxide radical (**TS4**), opening of the epoxide ring (**7** and **9**), and the final scission of the ring (**TS6** and **10**). The alternative path (**TS3**, **6**, and **TS7**) and the plausible side reaction (**TS5** and **8**) involve markedly higher barriers than those of the competing reactions of the proposed mechanism (see Figure 2).

Except for the initial dioxygen binding, the rest of the catalytic cycle takes place on the quintet potential energy surface (PES). His292 stays neutral throughout the catalytic cycle, which means that its role is limited to substrate binding at the HGD active site. The detailed discussion of the mechanism and the calculated energetics is presented in the following subsections.

Formation of the Peroxo Intermediate. The catalytic reaction of HGD starts with binding of molecular dioxygen to

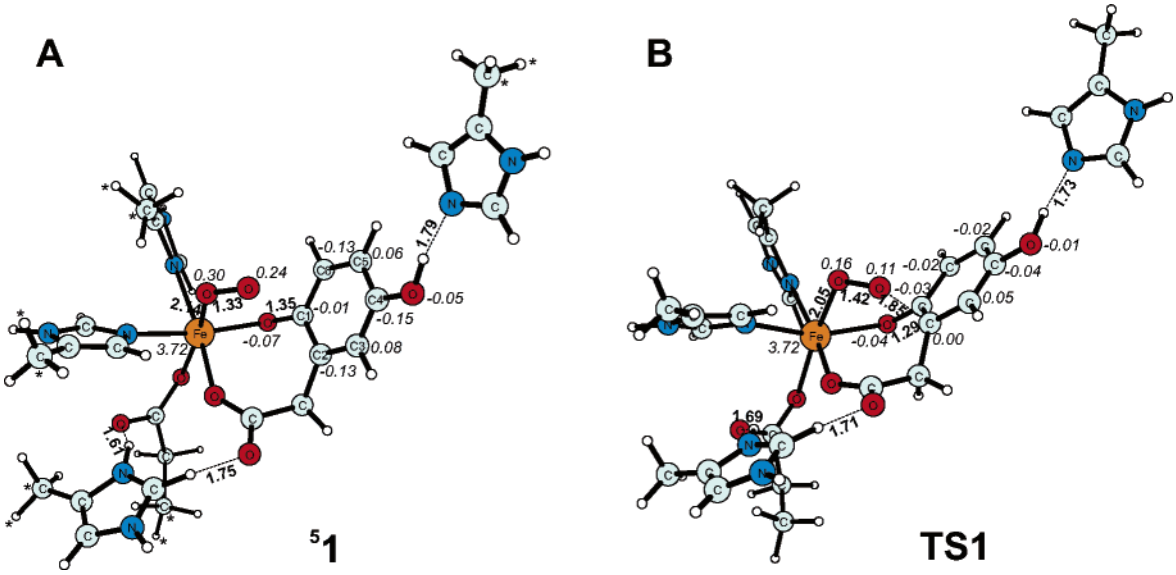

Figure 3. Optimized structures for: (A) quintet HGD-HG-O_2 complex ^{5}**1** (the positions of atoms marked with asterisks have been constrained in all geometry optimizations) and (B) transition state for an attack of the dioxygen ligand at the aromatic ring **TS1**. Distances in Å in bold, spin populations in italics.

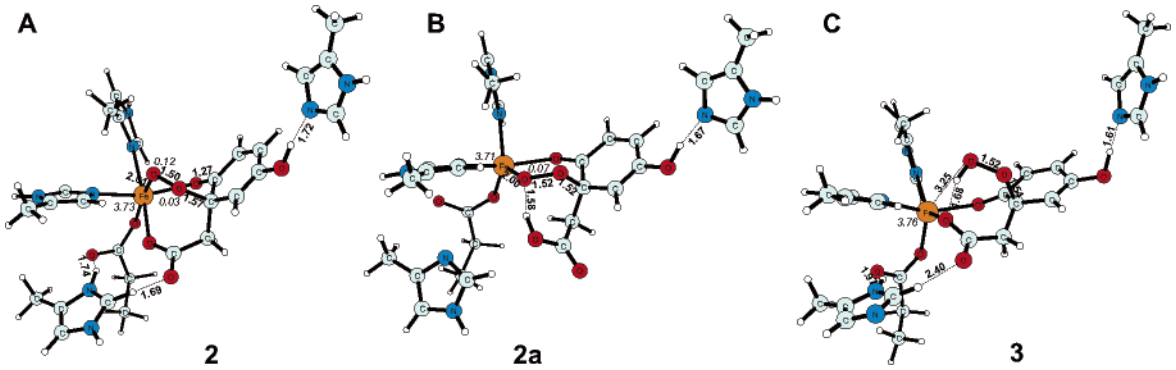

Figure 4. Optimized structures for: (A) peroxo-bridged intermediate **2**, (B) peroxo-bridged intermediate with a hydrogen bond between protonated carboxyl and peroxo groups **2a**, and (C) hydroperoxo species **3**. Distances in Å in bold, spin populations in italics.

the Fe^{II}−HGD−HG complex. Dioxygen binds to the active-site iron trans to Glu341. The ground state of the resulting ternary complex (HGD−HG−O_2) is a septet, which lies 1.1 kcal/mol above the zero level corresponding to separate reactants. However, as for many other Fe^{II}-dependent dioxygenases, the reactive state is the quintet.[36] Excitation to this state requires only 3 kcal/mol and leads to the structure ^{5}**1** presented in Figure 3A. From the spin populations reported one can notice that in this quintet complex HG has a substantial radical character, which is equivalent to the semiquinone intermediate proposed for extradiol dioxygenases.[37] Importantly, in the quintet ternary complex ^{5}**1** the total spin on the ring and the dioxygen fragment have opposite signs, which facilitates the formation of the bond between these two fragments of the complex.[28] Furthermore, on the quintet PES the high-spin configuration of Fe^{II} and Fe^{III} intermediates and products can be easily formed, which is also important, since the non-heme iron enzymes with oxygen and nitrogen donating ligands tend to have high-spin ground states. Thus, once the quintet PES is reached, the catalytic reaction of HGD continues on this potential energy surface.

The attack of the dioxygen fragment on the C2 carbon of the HG ring leads through the transition state **TS1** shown in Figure 3B. From the reported spin populations one can notice that the radical character of the HG ring and dioxygen fragment is being quenched at this step. Also from the bond lengths for **TS1** it can be recognized that the dioxygen fragment acquires a peroxo character, while the C1-bound phenolic group of HG turns into a ketone functionality. The spin population on iron remains unchanged, which indicates that the metal stays in the high-spin Fe^{II} state. The calculated activation barrier for the peroxo bridge formation amounts to 18.9 kcal/mol, which is the highest barrier along the suggested reaction path. Importantly, the barrier for an attack at the unsubstituted carbon (C6) is markedly higher, i.e., 23.4 kcal/mol which, together with other barriers discussed below, guarantees the proper product specificity of HGD. The observed preference for an attack at the C1 carbon is tentatively attributed to the fact that at the TS geometry the electron transfer from the ring to the dioxygen fragment is fairly advanced. Thus, at the transition state the bond forms between a peroxy anion and a carbocation. The latter is more stable if the charge accumulates on the ternary (C2), as opposed to the secondary (C6), carbon.

The peroxo-bridged structure (**2**), which is formed in the initial attack of the Fe-bound O_2 fragment on the aromatic ring,

(36) Bassan, A.; Borowski, T.; Siegbahn, P. E. M. *Dalton Trans.* **2004**, *20*, 3153−3162.

(37) Spence, E.; Langley, G.; Bugg, T. *J. Am. Chem. Soc.* **1996**, *118*, 8336−8343.

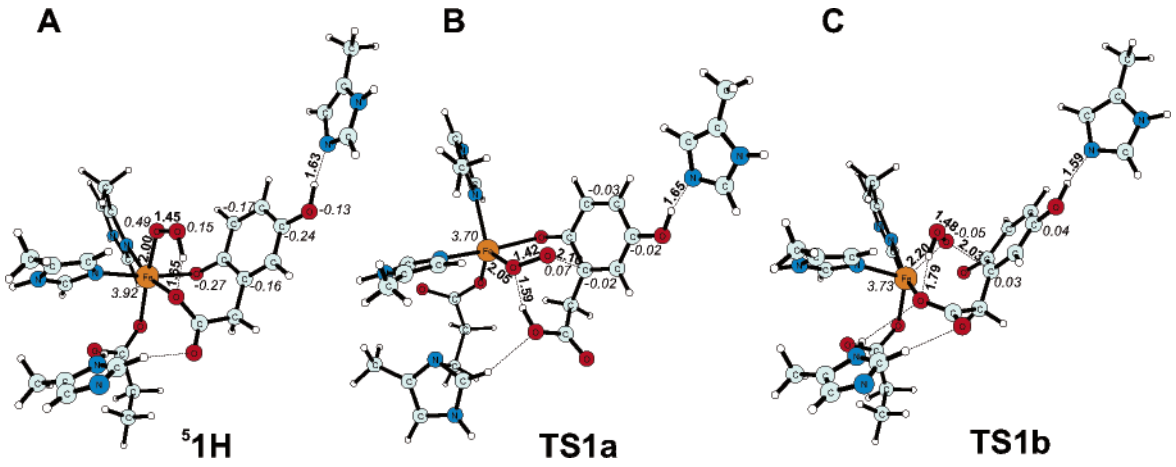

Figure 5. Optimized structures for: (A) quintet hydroperoxo species ^{5}**1H**, (B) transition state for a proton assisted attack on the ring **TS1a**, and (C) transition state for a transfer of the HOO radical between iron and the ring **TS1b**. Distances in Å in bold, spin populations in italics.

is presented in Figure 4A. From the bond lengths and spin populations it is easy to recognize that in **2** an organic peroxide chelates high-spin Fe^{II}. Since in this structure Fe^{II} has three negatively charged ligands, i.e. the carboxyl groups of Glu341 and HG and the peroxo group, the latter should be a rather strong base. Indeed, the ground state for the peroxo-bridged structure is species **2a**, which lies 6.4 kcal/mol above the zero level. In this structure, the proton has been moved from His365 to the carboxyl group of the substrate, and this protonated carboxylate forms a strong hydrogen bond with the distal oxygen of the peroxo group (see Figure 4B). The details of this proton shift reaction have not been studied here because there are many possible paths for this process, and considering its exothermicity (8.8 kcal/mol), it is believed to be very fast. The direct proton shift from the carboxyl to the peroxo group yields intermediate **3**, which is 3.1 kcal/mol less stable than **2a**. In Figure 4C one can notice that in the hydroperoxo structure the peroxo-iron bond is broken, and a hydrogen bond is established between the hydroperoxo and carboxyl groups of the substrate. The contact between iron and the hydroperoxide is reestablished during the O−O bond cleavage discussed in the next subsection.

The alternative reaction mechanism which leads to the bridging peroxo structure has been investigated. In this mechanism the reactant is the quintet species ^{5}**1H** (Figure 5A), which is formed from ^{5}**1** by a proton transfer from His365 to the distal oxygen of the O_2 ligand. The spin populations on iron and the HOO group show that this intermediate is a mixture of two resonance structures: $Fe^{III}-{}^{-}OOH$ and $Fe^{II}-{}^{\bullet}OOH$. The calculated energy of this species is −0.2 kcal/mol, which indicates that, as in the study of Deeth and Bugg,[27] this is the lowest-energy structure attainable for the ternary enzyme−substrates complex. Starting from this species two transition states for attack on the ring have been optimized. In the first one, **TS1a** (Figure 5B), the distal oxygen atom is deprotonated by the carboxyl group of the HG side chain and attacks the C2 carbon in the ring. This TS is similar to the one found by Deeth and Bugg. However, **TS1a** leads to the stable bridging peroxo structure **2a**, while the TS reported by Deeth and Bugg leads to the arene oxide intermediate. The calculated energy of **TS1a** is 19.2 kcal/mol, which is only 0.3 kcal/mol higher than the energy of **TS1**. In the second transition state, **TS1b** (Figure 5C), the distal oxygen atom of the OOH group remains protonated, while the proximal one detaches from iron and forms a bond with the C2 carbon. Thus, **TS1b** connects ^{5}**1H** with **3**. The calculated energy of **TS1b** is 18.3 kcal/mol, which is 0.6 kcal/mol less than the energy of **TS1**.

Taken together, there are at least three pathways which involve comparable barriers and lead to the bridging peroxo structure. The suggested mechanism for the decay of this species is discussed in the following section, while the less likely routes are presented at the end of this article.

O−O bond cleavage. The O−O bond in the hydroperoxo species undergoes an easy homolytic cleavage leading to the Fe^{III}−OH/alkoxyl radical species **4** (see Scheme 4). The calculated activation barrier is 10.7 kcal/mol, and the reaction (**2a** → **4**) is exothermic by 1.6 kcal/mol. The optimized transition state for this step (**TS2**) is presented in Figure 6A.

From the spin populations and bond lengths is can be recognized that the O−O bond cleavage is promoted by an electron transfer from Fe^{II} to the peroxo group. More specifically, for the transition-state geometry the negative spin population builds up on the oxygen atom bound to the ring, the spin population on iron increases, which indicates a depleted β spin density, and the Fe−OH bond is formed. In the metastable product of the homolytic O−O bond cleavage, i.e., **4**, these features are fully expressed (see Figure 6B). An analogous homolytic cleavage of an O−O bond yielding high-spin Fe^{III}−OH species has been proposed for activation of lipoxygenase.[38] Lipoxygenase is also a non-heme iron enzyme with an iron coordination sphere very similar to that of HGD.[39]

The product of the O−O bond homolysis, i.e., the alkoxyl radical species **4**, has been found to be a metastable species, since it collapses to the arene oxide radical intermediate **5** without any activation barrier (see Figure 2). In the previous study on extradiol dioxygenases a small activation barrier (0.2 kcal/mol) was found for an equivalent reaction.[28] The arene oxide radical intermediate (**5**) lies 26.1 kcal/mol below the peroxo-bridged structure, and due to this big energy difference the O−O bond cleavage is practically irreversible.

The high stability of **5** can be understood from its structure presented in Figure 7A. From the spin populations one can

(38) Kulkarni, A. *Cell. Mol. Life Sci.* **2001**, *58*, 1805−1825.
(39) Minor, W.; Steczko, J.; Stec, B.; Otwinowski, Z.; Bolin, J.; Walter, R.; Axelrod, B. *Biochemistry* **1996**, *35*, 10687−10701.

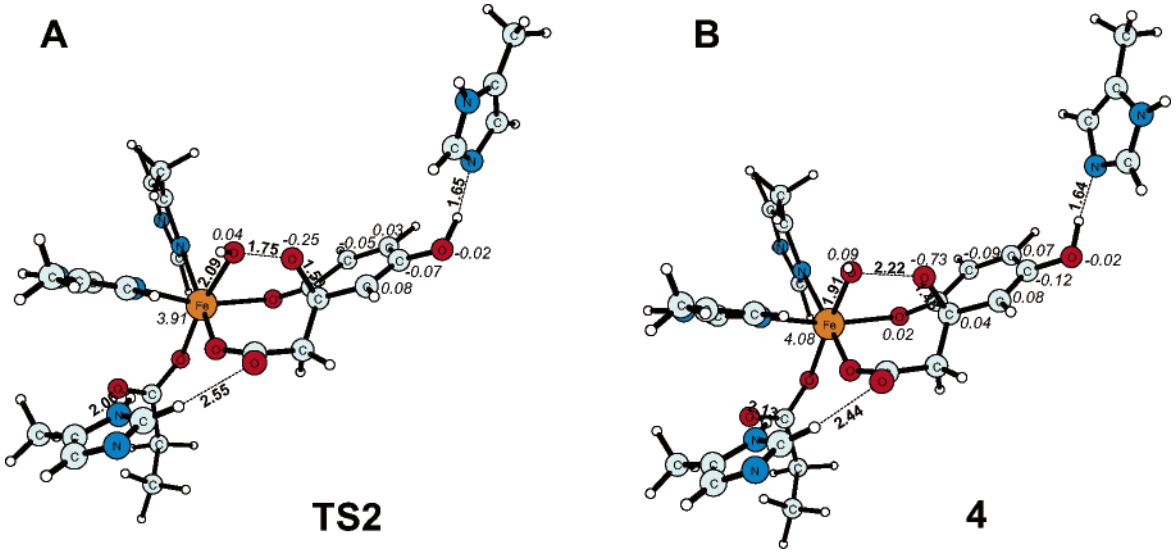

Figure 6. Optimized structures for: (A) transition state for O−O bond cleavage **TS2** and (B) metastable radical species **4**. Distances in Å in bold, spin populations in italics.

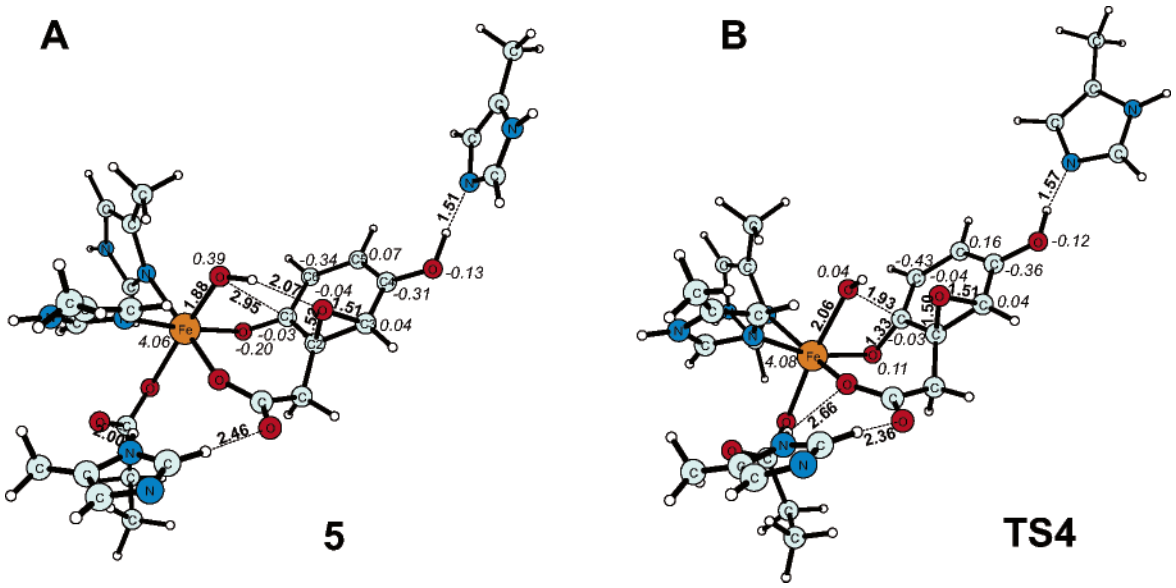

Figure 7. Optimized structures for: (A) arene oxide radical species **5** and (B) transition state (**TS4**) for a nucleophilic attack of the Fe-bound OH group on the carbonyl carbon (C1). Distances in Å in bold, spin populations in italics.

notice that all three radical resonance structures which can be drawn for **5** contribute to its electronic structure. Accordingly, the unpaired spin is almost equally distributed among the carbons C4 and C6 and the iron-bound oxygen. Another feature of **5** is the proximity of the Fe^{III}-bound OH group and the carbonyl carbon of the ring (2.95Å). This is a structural hallmark of the reaction discussed in the next subsection.

The Fate of the Arene Oxide Radical. The short distance between the Fe-bound hydroxyl group and the carbonyl carbon in the intermediate **5** suggests that a nucleophilic attack at this position should be straightforward. Indeed, the calculated activation barrier is only 6.5 kcal/mol, and the reaction is endothermic by 4.3 kcal/mol. The optimized transition state (**TS4**) is shown in Figure 7B. Interestingly, even though in this reaction a four-membered ring is formed, the activation barrier is low. Already for the **TS4** geometry one can notice that a spin population on the carbonyl oxygen changes sign to positive. The magnitude of this spin population increases to 0.26 in the product of this reaction (**7**) shown in Figure 8A.

From the bond lengths for **7** one can notice that the weak Fe−OH bond is compensated by the relatively short bond between iron and the C1-bound oxygen (1.95 Å). The spin population on iron (4.05) still suggests a high-spin Fe^{III} species. Due to the addition of the OH group into the carbonyl functionality, intermediate **7**, compared to **5**, has one less resonance structure, and the unpaired spin density is distributed between carbons C4 and C6. Thus, starting from structure **7** it should be easier to open the epoxide ring than in the case of structure **5** opening back to **4**. Indeed, the metastable structure with opened epoxide ring (**9**) lies only 8.1 kcal/mol above **5**, which should be compared to the energy splitting of 24.5 kcal/mol between **5** and **4**. However, it is probable that aside from the difference in the number of resonance structures, a better hydrogen bonding between the OH group and the alkoxyl radical also contributes

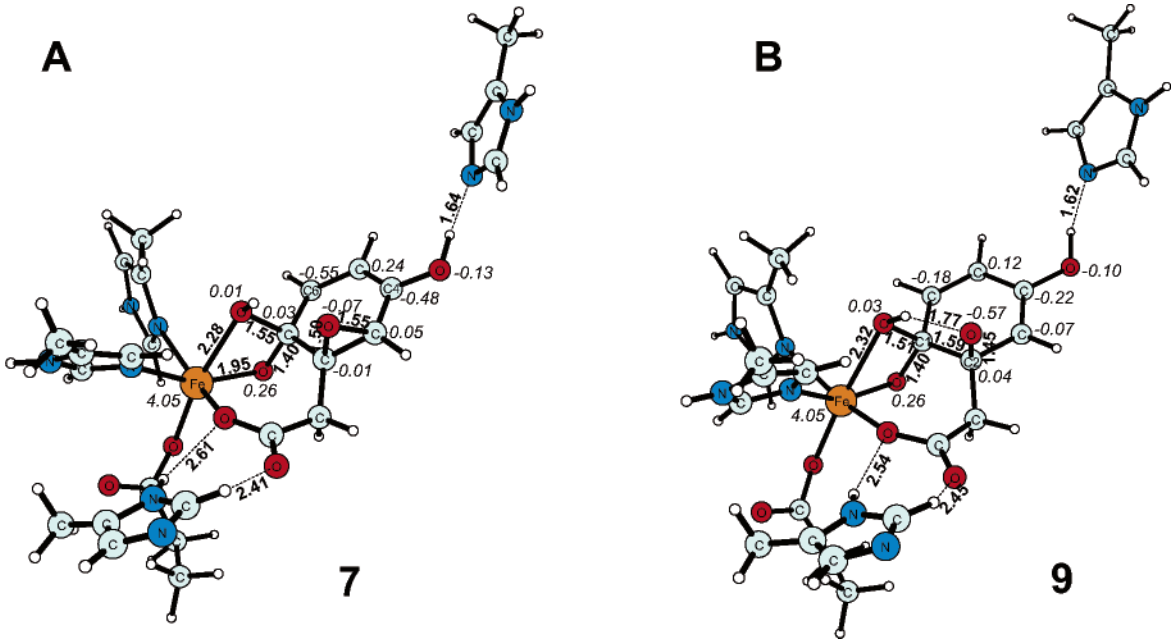

Figure 8. Optimized structures for: (A) intermediate **7** and (B) metastable species **9**. Distances in Å in bold, spin populations in italics.

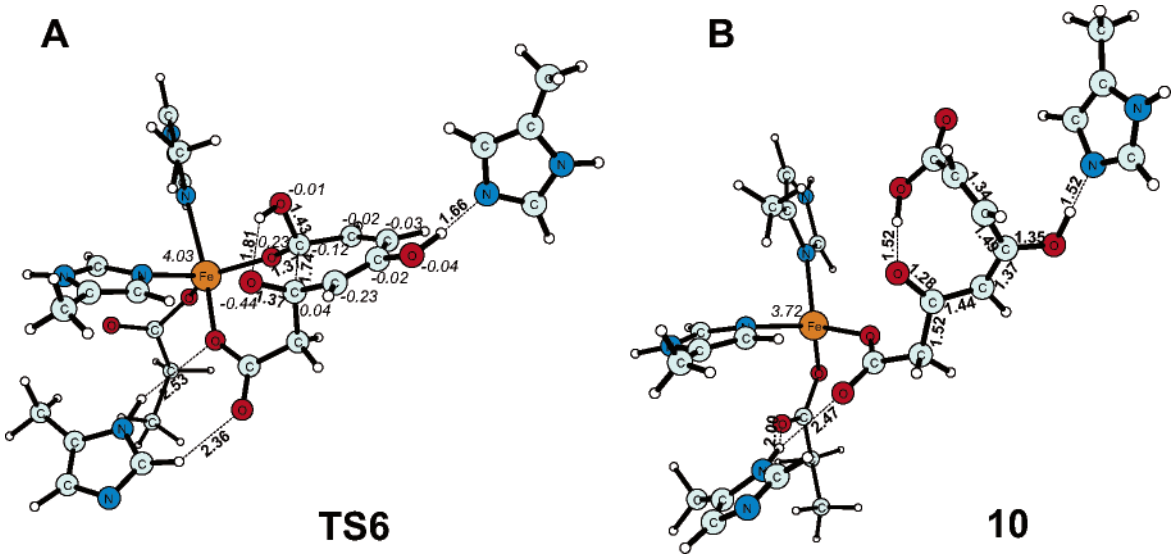

Figure 9. Optimized structures for: (A) transition state for the final ring scission **TS6** and (B) complex between the HGD active site and the enolic form of the product **10**. Distances in Å in bold, spin populations in italics.

to this relative stabilization (compare Figures 7A and 8B). Once the epoxide ring is opened, both carbon atoms flanking the bond to be cleaved, i.e., C1 and C2, have all necessary groups bound to them, and only a single bond scission is necessary to form the final product of the reaction. Notably, already in **9** the C1−C2 bond distance is elongated to 1.59 Å.

The optimized transition state for the final ring scission (**TS6**) is shown in Figure 9A. From the bond lengths one can notice that this transition state has a very early character, e.g. the C1−C2 bond length is only 1.74 Å. Moreover, concertedly with C1−C2 bond elongation the bonds between these carbon atoms and oxygens bound to them shorten markedly, which indicates formation of double bonds between these atoms. Concerning the energetics, the relative energy of **TS6** is −7.4 kcal/mol, which means that the accumulated barrier calculated with respect to the arene oxide radical **5** is 12.3 kcal/mol. It seems likely, that this relatively low activation energy stems partly from the fact that the ring is highly activated for cleavage by having three oxygen atoms bound to two adjacent carbons and partly from the very high exothermicity of this process. The calculated reaction energy for the transformation of **5** into **10** is −60 kcal/mol. The structure of the product complex is presented in Figure 9B. From the spin populations one can recognize that the ring has been cleaved to the closed-shell enolic form of maleylacetoacetate, while the active-site iron is back in the high-spin Fe^{II} electronic state. Since at this stage ring scission is completed and the active-site iron is again in its native oxidation state, it is suggested that complex **10** dissociates, probably with the help of some solvent molecules, into the product and the holo-enzyme ready for binding of HG and O_2 and for catalyzing the next cycle of the enzymatic reaction.

Side Reactions. In Scheme 4 it can be noticed that in addition to the suggested reaction mechanism, there are two alternative

Scheme 5. Alternative Mechanism of the Catalytic Reaction of HGD

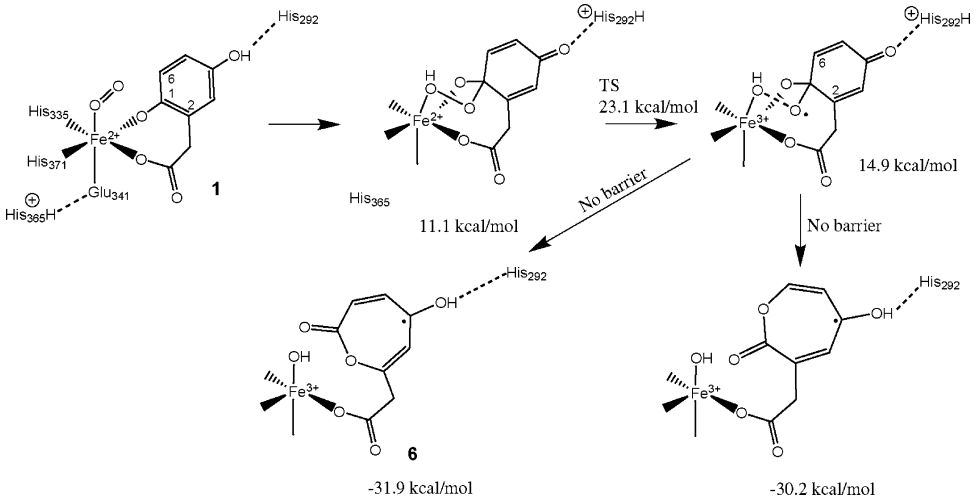

paths starting with the radical species **4** and **5**. In passing, it seems worthy to note that a similar branching of the reaction at the radical state was found in the study on 4-HPPD, an enzyme preceding HGD in the tyrosine metabolic pathway.[40] Thus, the first alternative reaction starts with **4** undergoing an alkoxyl radical insertion into the C1−C2 bond, i.e. the transformation **4** → **TS3** → **6** (for structures, see Supporting Information). This reaction involves an activation barrier of 2.6 kcal/mol. Even though this number is quite small, the competing reaction along the suggested path, i.e., the formation of the arene oxide radical (**4** → **5**), involves no activation barrier and is very exothermic. Therefore, it is suggested that the reaction channel involving **6** is not utilized by HGD. Nevertheless, the transition state (**TS7**) connecting **6** and the final product **10** has been optimized (for structure, see Supporting Information). In this step, the iron-bound OH group performs a nucleophilic attack at the carbonyl group of the lactone radical, which leads to opening and oxidation of the ring. The activation barrier for this reaction is 15.3 kcal/mol, which is 3 kcal/mol higher than the activation energy for a nucleophilic attack at the arene oxide radical (**5** → **TS4** → **7**). Finally, it should be noted that, while this reaction path is not very likely, it still leads to the observed product, maleylacetoacetate. In contrast, the second alternative reaction path leads to the product which is not observed experimentally. In this process, **5** → **TS5** → **8**, the C−C bond of the epoxide ring is cleaved, which leads to an oxepine radical. However, the barrier calculated for this step (19.6 kcal/mol) is substantially higher than the accumulated barrier for a productive decay along the suggested reaction path (**5** → **TS6**; 12.3 kcal/mol), and thus the products of this side reaction should not be observed.

Alternative Mechanisms. One alternative mechanism of the catalytic reaction of HGD involves an attack of the Fe-bound dioxygen on carbon C1, as opposed to the attack on C2 in the suggested mechanism discussed above (see Scheme 5). Even though this path has not been fully explored, already from the data presented in Scheme 5 some conclusions can be drawn. The first step of this reaction involves a formation of a hydroperoxo species. This process requires that the proton of the C4-bound hydroxyl group is moved to His292, while the proton originally bound to His365 is relocated to the peroxo group. Notably, the species with an unprotonated peroxo bridge is not stable, and during geometry optimization decomposes into the reactant. Due to the complicated nature of this first step, no attempts have been made to locate the appropriate transition-state structure(s). The next step is a homolytic cleavage of the O−O bond in the hydroperoxo species. This process involves an accumulated barrier of 23.1 kcal/mol, which is 4.8 kcal/mol higher than the rate-limiting barrier in the preferred mechanism (**TS1b**; 18.3 kcal/mol). The alkoxyl radical produced in the O−O homolysis is a highly reactive metastable species which spontaneously and irreversibly decays into two lactone radical intermediates. While one of these lactones (**6**) can be relatively easily transformed into maleylacetoacetate, the formation of the other leads to a ring-cleavage product which is not observed. In the optimized structure of the metastable radical species the two carbon−oxygen distances critical for the ring cleavage, (C6,C2)−oxo, are not equal; they are 2.14 and 2.46 Å for C6 and C2, respectively. Thus, this asymmetry should favor the formation of the "wrong" product. Taken together, this alternative mechanism involves a markedly higher activation barrier and cannot explain the observed product specificity of HGD; therefore, it is considered to be unlikely.

The second alternative mechanism which has been tested is the Criegee rearrangement shown in Scheme 3. First, several attempts have been made to optimize the structure of the product of a Criegee rearrangement, i.e., the complex with Fe^{II}-bound OH group and the closed-shell lactone. However, all these calculations notoriously converged to the structure with Fe^{III}−OH and a lactone radical, which indicates that Fe^{II} coordinated by three negatively charged ligands, i.e., two carboxylates and OH, is easily oxidized by such a lactone. Therefore, it is concluded that for the Criegee rearrangement it is necessary that the leaving OH group is not supported by iron, since such an Fe−OH interaction promotes a radical mechanism. One plausible arrangement which would lead to Criegee rearrangement includes a protonated carboxylic group of the substrate (see Scheme 6A). In such a structure, the leaving OH group is protonated by the carboxylic functionality, and no contact between Fe and OH is necessary. Therefore, it might be expected that the presence of the spectator iron ion is not critical for such a reaction, and first, the Criegee rearrangement was studied with a smaller model not involving the metal (see Scheme 6A and

(40) Borowski, T.; Bassan, A.; Siegbahn, P. E. M. *Biochemistry* **2004**, *43*, 12331−12342.

Scheme 6. Proton-Assisted Criegee Rearrangement for HGD

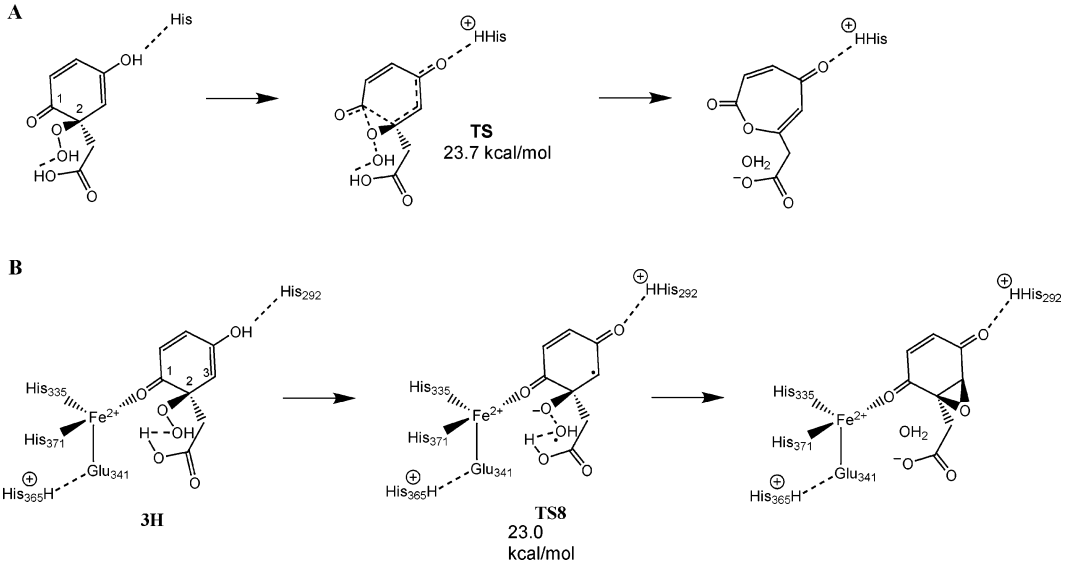

Scheme 7. Alternative Mechanism Involving Dioxethane-Like Transition State

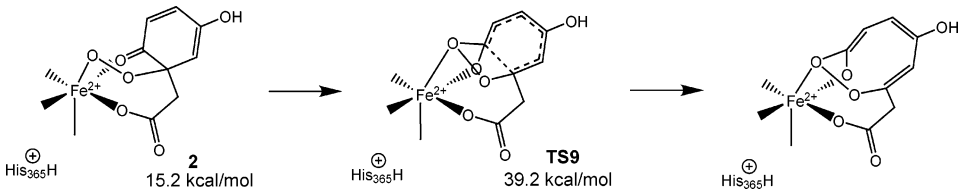

Figure S5). For this model, the closed-shell singlet transition state connecting the peroxo species with the lactone was optimized, and the imaginary frequency corresponding to the reaction coordinate shows that concertedly with the O−O bond cleavage and oxygen insertion into the ring two protons are transferred, one to the leaving OH group and another to the histidine model (Figure S5). Thus, this transition state corresponds to the Criegee rearrangement. However, the calculated barrier for this reaction is 23.7 (with the solvent effects 29.6 kcal/mol), which is much larger than the barrier for homolytic O−O bond cleavage in the above suggested catalytic mechanism of HGD (**2a** → **TS2**, 10.7 kcal/mol). The geometry of this TS has been used as a starting point in the optimization of the corresponding TS in the model comprising the active-site iron and the surrounding protein ligands (see Scheme 6B and Figure S6). However, the spin-unrestricted calculations, motivated by the presence of the iron ion, converged to the structure **TS8** (Scheme 6), where the O−O cleavage is homolytic in nature, the ring is one-electron oxidized, and there is no sign of oxygen atom insertion into the ring. Notably, the energy of **TS8** is slightly lower than the energy of the optimized TS for Criegee rearrangement in the smaller model, but still much larger than the energy of **TS2**. Thus, it is concluded that the TS for Criegee rearrangement could not be optimized with the model involving iron because the homolytic process involves a lower activation energy. These results indicate that a Criegee rearrangement is not likely to account for the catalytic reaction of HGD.

Finally, the mechanism involving a dioxethane-like transition state (see Scheme 7 and Figure S7) has been tested, but the energy of such a TS (**TS9**; 39.2 kcal/mol) is prohibitively high. In this mechanism, the C−C bond cleavage precedes the O−O scission. Taken together, the alternative mechanisms for the HGD catalytic reaction involve higher activation barriers than the mechanism suggested in this work, and in the case of the mechanism shown in Scheme 5 lead to products not observed experimentally.

Conclusions

The computational results suggest that HG coordinates the HGD active-site iron in such a manner that the position trans to Glu341 remains empty. Dioxygen binds to iron at this position, and once the ternary complex reaches the quintet PES, the catalytic reaction involves three major chemical steps. First, the iron-bound dioxygen attacks the aromatic ring at the C2 carbon (**1** → **TS1** → **2**, see Scheme 4). Importantly, the attack at C6 or C1 leads to markedly higher barriers. Second, the peroxo species is protonated by His365 and undergoes a homolytic O−O bond cleavage (**2** → **3** → **TS2** → **4** → **5**). This relatively easy and practically irreversible reaction leads to an arene oxide radical **5**. Finally, a nucleophilic attack of the Fe-bound OH group on the carbonyl carbon of **5** (**5** → **TS4** → **7**) activates the six-membered ring for cleavage. This last process involves an opening of the epoxide ring (**7** → **9**) and the final C1−C2 bond scission leading to maleylacetoacetate (**9** → **TS6** → **10**). Notably, an alternative manner of epoxide ring opening, which leads to an oxepine radical (**5** → **TS5** → **8**) involves a substantially higher barrier.

The suggested mechanism for the catalytic reaction of HGD agrees with several experimental observations for extradiol dioxygenases. First, the dioxygenase nature of HGD is guaranteed by this mechanism, since both atoms of O_2 are inserted into the product. Moreover, the intermediacy of the Fe^{III}−OH species opens up the possibility for an oxygen atom exchange with water, which has been observed for some extradiol dioxygenases.[26] In addition, several intermediates have radical character with an unpaired electron in the π orbital of the ring,

and such intermediates were postulated on the basis of the identity of the products obtained for a radical clock substrate.[37] Finally, the second hydroxyl group of the substrate, in the case of HG bound to C4, except for participating in proper binding of HG in the active site does not play any active role in the catalytic reaction, which is in line with the observed activity of salicylate 1,2-dioxygenase catalyzing a ring scission in a substrate lacking such a group.[11,12] Taken together, it is believed that the mechanism suggested here has a sound basis and may stimulate further research aimed at understanding the catalytic mechanism of HGD and other Fe^{II}-dependent ring-cleaving enzymes.

Acknowledgment. We are grateful to Sven de Marothy for providing us with his XYZ-Viewer program which was used to produce the molecular graphics presented in this manuscript. T.B. acknowledges the support from the Polish State Committee for Scientific Research (Grant 2 P04A 042 26).

Supporting Information Available: Full author list for reference 31; Cartesian coordinates and calculated energies for all ground and transition state structures; Figure S1 with two orthogonal views of the complex from Figure 1A in VDW representation, Figure S2 showing superimposed active-site regions of two homoprotocatechuate 2,3-dioxygenase crystal structures: 1F1X and 1Q0C, Figure S3 presenting the structures of **TS3** and **6**, Figure S4 presenting **TS5**, **TS7**, and **8**, Figure S5 with the reactant and TS for Criegee rearrangement (small model), Figure S6 with the structures of **3H** and **TS8**, and Figure S7 showing **TS9**. This material is available free of charge via the Internet at http://pubs.acs.org.

JA054433J